

Haptoglobin-2 variant increases susceptibility to the acute respiratory distress syndrome during sepsis

V. Eric Kerchberger, ... , Edward D. Siew, Lorraine B. Ware

JCI Insight. 2019. <https://doi.org/10.1172/jci.insight.131206>.

Research In-Press Preview Genetics Pulmonology

The acute respiratory distress syndrome (ARDS) is an inflammatory lung disorder that frequently complicates critical illness, and most commonly occurs in the setting of sepsis. Although a number of clinical and environmental risk factors for ARDS have been described, not all patients with risk factors develop the syndrome, raising the possibility of genetic underpinnings for ARDS susceptibility. We have previously reported that circulating cell-free hemoglobin (CFH) is elevated during sepsis, and higher levels are associated with worse outcomes. CFH is rapidly scavenged by the plasma protein haptoglobin (Hp). A common *HP* genetic variant *HP2* is unique to humans and represents 60% of the *HP* allele frequency in populations of European ancestry. The *HP2* gene product has reduced ability to inhibit CFH-mediated inflammation and oxidative stress compared to the alternative *HP1*. We hypothesized that the *HP2* variant increases ARDS susceptibility during sepsis when plasma CFH levels are elevated. In a murine model of sepsis with elevated CFH levels, transgenic mice homozygous for *Hp2* had increased lung inflammation, pulmonary vascular permeability, lung apoptosis, and mortality compared to mice homozygous for the alternative allele *Hp1*. We then tested the clinical relevance of our findings in a prospective observational cohort study of 496 septic critically ill adults, and found that the *HP2* variant was significantly associated with increased ARDS susceptibility (odds ratio 1.41 per [...])

Find the latest version:

<https://jci.me/131206/pdf>



Haptoglobin-2 variant increases susceptibility to the acute respiratory distress syndrome during sepsis

V. Eric Kerchberger,^{1,2} Julie A. Bastarache,^{1,3,4} Ciara M. Shaver,¹ Hiromasa Nagata,⁵
J. Brennan McNeil,¹ Stuart R. Landstreet,¹ Nathan D. Putz,¹ Wen-Kuang Yu,^{1,6}
Jordan Jesse,¹ Nancy E. Wickersham,¹ Tatiana N. Sidorova,¹ David R. Janz,⁷
Chirag R. Parikh,⁸ Edward D. Siew,⁹ and Lorraine B. Ware^{1,4}

1) Division of Allergy, Pulmonary, and Critical Care Medicine, Department of Medicine, Vanderbilt University Medical Center, Nashville, Tennessee, USA

2) Department of Biomedical Informatics, Vanderbilt University Medical Center, Nashville, Tennessee, USA

3) Department of Cell and Developmental Biology, Vanderbilt University, Nashville, Tennessee, USA

4) Department of Pathology, Microbiology and Immunology, Vanderbilt University Medical Center, Nashville Tennessee, USA

5) Department of Anesthesiology, Keio University School of Medicine, Tokyo, Japan

6) Department of Chest Medicine, Taipei Veterans General Hospital, Taipei, Taiwan, School of Medicine, National Yang-Ming University, Taipei, Taiwan

7) Section of Pulmonary and Critical Care Medicine, Louisiana State University School of Medicine, New Orleans, Louisiana, USA

8) Division of Nephrology, Department of Medicine, Johns Hopkins University School of Medicine, Baltimore, Maryland, USA.

9) Division of Nephrology and Hypertension, Department of Medicine, Vanderbilt University Medical Center, Nashville, Tennessee, USA

Corresponding Author:

Lorraine B. Ware, MD

Division of Allergy, Pulmonary, and Critical Care Medicine

Vanderbilt University Medical Center

1161 21st Ave South

T-1218, Medical Center North

Nashville, TN 37232

Phone: 615-322-7872

Email: lorraine.ware@vumc.org

Conflict of Interest Statement: Dr. Ware reports consulting fees from CSL Behring, Bayer and Quark Pharmaceuticals as well as a research contract with CSL Behring (current) and past research contracts with Boehringer Ingelheim and Global Blood Therapeutics, all unrelated to the current manuscript. Dr. Parikh is a named inventor on provisional patent number 62/716,465 titled "System and methods for diagnosing acute interstitial nephritis" which is unrelated to the current manuscript. The remaining authors have declared that no conflicts of interest exist.

48 **Abstract**

49 The acute respiratory distress syndrome (ARDS) is an inflammatory lung disorder that
50 frequently complicates critical illness, and most commonly occurs in the setting of sepsis.
51 Although a number of clinical and environmental risk factors for ARDS have been described,
52 not all patients with risk factors develop the syndrome, raising the possibility of genetic
53 underpinnings for ARDS susceptibility. We have previously reported that circulating cell-free
54 hemoglobin (CFH) is elevated during sepsis, and higher levels are associated with worse
55 outcomes. CFH is rapidly scavenged by the plasma protein haptoglobin (Hp). A common *HP*
56 genetic variant *HP2* is unique to humans and represents 60% of the *HP* allele frequency in
57 populations of European ancestry. The *HP2* gene product has reduced ability to inhibit CFH-
58 mediated inflammation and oxidative stress compared to the alternative *HP1*. We
59 hypothesized that the *HP2* variant increases ARDS susceptibility during sepsis when plasma
60 CFH levels are elevated. In a murine model of sepsis with elevated CFH levels, transgenic
61 mice homozygous for *Hp2* had increased lung inflammation, pulmonary vascular permeability,
62 lung apoptosis, and mortality compared to mice homozygous for the alternative allele *Hp1*.
63 We then tested the clinical relevance of our findings in a prospective observational cohort
64 study of 496 septic critically ill adults, and found that the *HP2* variant was significantly
65 associated with increased ARDS susceptibility (odds ratio 1.41 per *HP2* allele, 95%
66 confidence interval 1.06 – 1.88, $P = 0.018$) after controlling for clinical risk factors and plasma
67 CFH. This relationship between the *HP2* genetic variant and ARDS risk was only seen in
68 patients with elevated plasma CFH levels. These observations identify the *HP2* variant as a
69 novel genetic ARDS risk factor during sepsis, and may have important implications in the
70 study and treatment of ARDS.

71 **Introduction**

72 The acute respiratory distress syndrome (ARDS) is an acute inflammatory lung disorder that
73 frequently complicates critical illness and affects over 200,000 adults per year in the United
74 States (1–3). Despite decades of research, currently there are no disease-modifying
75 treatments that reduce ARDS mortality (4–6). The majority of patients with ARDS clinical risk
76 factors do not develop the syndrome, and there is substantial variability in disease severity
77 among patients who do develop ARDS (4, 7). This suggests that additional factors including
78 inheritable genetic factors may contribute to ARDS susceptibility (4, 8).

79

80 Sepsis, a clinical syndrome characterized by dysregulated inflammation and organ
81 dysfunction in response to infection, is the most common cause of ARDS (1–3, 9, 10).

82 Patients with sepsis have alterations in red blood cell (RBC) membrane stability resulting in
83 hemolysis (11–14). Hemoglobin released from RBCs, termed cell-free hemoglobin (CFH), is
84 detectable in the plasma of 80% of critically ill sepsis patients (15), and higher plasma CFH
85 levels are associated with increased organ dysfunction and mortality during sepsis (15, 16).
86 CFH causes organ injury via scavenging of nitric oxide in vascular beds (17), injury to the
87 vascular endothelium (18), neutrophil activation (19), and oxidation of lipid cell membranes
88 (20, 21). Therefore, elevated plasma CFH during sepsis may contribute to development of
89 ARDS.

90

91 The plasma protein haptoglobin (Hp) serves as the primary endogenous scavenger for CFH
92 in mammals (22). Hp binds irreversibly to CFH, and the resultant CFH-Hp complex binds with
93 high affinity to the CD163 receptor present on monocytes and macrophages (23), resulting in

94 endocytosis and clearance of CFH from the circulation (24, 25). Humans have a unique *HP*
95 genetic variant *HP2* (26), which comprises 45% of the *HP* allele frequencies in African-
96 American and west African populations, 60% in European populations, and 75% in East and
97 South Asian populations (27). Hp from subjects homozygous for the *HP2* variant (*HP2-2*
98 genotype) has reduced ability to inhibit CFH-mediated inflammation and oxidative stress
99 compared with Hp from subjects homozygous for the alternative allele *HP1* (*HP1-1* genotype)
100 (25, 28, 29). The *HP2-2* genotype has been associated with increased risk of atherosclerotic
101 coronary artery disease (30, 31), diabetic nephropathy (32, 33), and worse outcomes after
102 subarachnoid hemorrhage (34, 35).

103

104 We hypothesized that the *HP2* variant increases susceptibility to ARDS in the setting of
105 sepsis with elevated CFH, as Hp in patients with the *HP2* variant would be predicted to have
106 reduced ability to mitigate CFH-mediated oxidative stress and inflammation. Utilizing
107 transgenic mice with a murine homologue of human *HP2*, we determined the mechanistic
108 effects of *HP2* on acute lung injury in an experimental model of polymicrobial sepsis, finding
109 that *Hp2-2* mice experienced increased lung inflammation, pulmonary vascular endothelial
110 injury, and mortality compared to wild-type *Hp1-1* mice. We then validated our observations in
111 a prospective observational cohort study of septic critically ill adults, finding that the *HP2*
112 variant was significantly and independently associated with increased susceptibility to ARDS
113 in humans. These findings identify the *HP2* variant as a novel genetic risk factor for ARDS
114 during sepsis.

115 **Results**

116 ***Hp2-2* mice have decreased survival during experimental sepsis**

117 We first tested the effect of *Hp* genotype on survival in a murine model of polymicrobial sepsis
118 with elevated CFH levels. Following injection of intraperitoneal cecal slurry (CS) and
119 intravenous CFH, *Hp2-2* mice had decreased survival compared with *Hp1-1* mice ($P = 0.03$
120 by log-rank test, **Figure 1, Panel A**). Although median plasma CFH levels were higher in
121 *Hp2-2* mice compared with *Hp1-1* mice, these differences did not reach statistical significance
122 ($P = 0.09$ by Mann-Whitney *U* test, **Figure 1, Panel B**).

123

124 ***Hp2-2* mice have increased lung inflammation during experimental sepsis**

125 We next assessed the effect of *Hp* genotype on lung inflammation in the mouse polymicrobial
126 sepsis model. *Hp2-2* mice had increased lung inflammation compared with *Hp1-1* mice in
127 response to intraperitoneal CS and intravenous CFH, as evidenced by increased whole lung
128 myeloperoxidase activity ($P = 0.014$, **Figure 2, Panel A**) and CXCL-1 mRNA expression ($P =$
129 0.022 , **Figure 2, Panel B**). *Hp2-2* mice also had increased CXCL-1 levels in BAL fluid
130 compared with *Hp1-1* mice ($P = 0.011$, **Figure 2, Panel C**).

131

132 ***Hp2-2* mice have increased pulmonary vascular permeability and lung apoptosis**
133 **during experimental sepsis**

134 We next tested the effects of *Hp2-2* genotype on the pulmonary vascular endothelium,
135 hypothesizing that CFH may impair pulmonary vascular barrier function during sepsis. We
136 tested microvascular barrier integrity by retro-orbital injection of AngioSense[®], a 70-kDa near-
137 infrared fluorescent macromolecule that accumulates in sites of increased vascular

138 permeability. *Hp2-2* mice had increased lung accumulation of AngioSense® compared with
139 *Hp1-1* mice twenty-four hours after intraperitoneal CS and IV CFH ($P = 0.037$, **Figure 3**). This
140 finding indicates that *Hp2-2* mice have worsened pulmonary vascular permeability during
141 sepsis compared with *Hp1-1* mice. Excised lungs from *Hp2-2* mice also had increased
142 apoptosis by TUNEL staining compared with lungs from *Hp1-1* mice ($P = 0.004$, **Figure 4**).
143 We have previously determined that 80% of apoptotic lung cells in this CS + CFH model are
144 endothelial using co-labeling in samples from wild type mice (Bastarache JA, et al.,
145 unpublished observations). Therefore, this suggests that lung endothelial apoptosis
146 contributes to increased microvascular permeability in this model.

147

148 **Adult sepsis cohort haptoglobin genotyping**

149 To examine the clinical implications of the mechanistic findings from the mouse polymicrobial
150 sepsis model, we tested the association between *HP* genotype and ARDS in a prospective
151 observational cohort of critically ill adults hospitalized with sepsis. We determined *HP*
152 genotype by two different methods depending on data and sample availability. For the 344
153 patients in whom DNA was available, we directly genotyped *HP* using real-time PCR. In an
154 additional 152 patients, we used prior GWAS level genotyping to impute *HP* genotype using a
155 previously reported algorithm (36). To verify the accuracy of the imputation method in our
156 cohort, we determined genotype by both methods in 120 patients. The observed *HP* genotype
157 distribution in the entire study cohort ($N = 496$) was 15% *HP1-1*, 45% *HP2-1*, and 40% *HP2-2*
158 (**Supplemental Figure 1**). The observed *HP* genotype distribution was similar to expected
159 allele frequencies for a majority-European ancestry cohort (27) ($P = 0.12$ for difference from
160 reference *HP2* allele frequency by two-sample binomial proportions test). The overall

161 agreement between PCR and imputation in the 120 patients genotyped by both methods was
162 0.91 (Cohen's Kappa 0.85, balanced accuracy 0.91, 95% CI [0.84, 0.95]) (**Supplemental**
163 **Table 1, Supplemental Figure 2**).

164

165 **Adult sepsis cohort patient clinical characteristics**

166 Patients with all three *HP* genotypes had similar baseline clinical characteristics including
167 age, sex, reported ethnicity, comorbid medical conditions, APACHE II scores, mechanical
168 ventilation on enrollment, and organ failures as measured by Brussels score (37) (**Table 1**).
169 Plasma CFH levels measured on ICU day 2 were similar across all three genotypes, while
170 plasma Hp levels were significantly decreased in *HP2-1* and *HP2-2* patients compared with
171 *HP1-1* ($P = 0.0008$ by Kruskal-Wallis test, **Table 1, Supplemental Figure 3**), consistent with
172 prior epidemiological studies of serum Hp levels among different *HP* genotypes (38, 39).

173

174 **Elevated circulating cell-free hemoglobin increases risk of ARDS**

175 During the first four ICU days, 181 (36.5%) patients developed ARDS. To test the hypothesis
176 that *HP* genotype modulates the effect of CFH on ARDS susceptibility, we first tested the
177 association between plasma CFH levels and ARDS susceptibility. We observed a dose-
178 response relationship between plasma CFH and increased risk for ARDS ($P = 0.032$ by
179 Cochran-Armitage test for increasing ARDS risk by CFH quartile, **Figure 5**).

180

181 **Haptoglobin 2 variant increases ARDS risk in critically ill adults with sepsis**

182 The distribution of ARDS cases among genotypes was *HP1-1* 28.9% ($N = 22$), *HP2-1* 35.3%
183 ($N = 79$), and *HP2-2* 40.8% ($N = 80$). In the unadjusted analysis, ARDS risk significantly

184 increased with increasing number of *HP2* alleles. Compared with *HP1-1* genotype, *HP2-1* had
185 an odds ratio (OR) for ARDS of 1.33, and *HP2-2* had an OR for ARDS of 1.68, with $P = 0.029$
186 by the Cochran-Armitage test for increasing ARDS risk ordered by number of *HP* alleles
187 (**Figure 6**). To test whether the relationship between *HP* genotype and ARDS was mediated
188 by CFH, we assessed the impact of *HP* genotype in the presence and absence of detectable
189 CFH. The association between *HP* genotype and ARDS susceptibility was present only in
190 patients with detectable levels of plasma CFH ($P = 0.026$, $N = 414$), and not in patients with
191 undetectable levels of plasma CFH ($P = 0.46$, $N = 82$) (**Figure 7**).

192

193 **Haptoglobin 2 variant is an independent ARDS risk factor**

194 To control for prespecified clinical confounders, we tested the association of *HP* genotype with
195 ARDS using a multivariable logistic regression model. *HP* genotype remained independently
196 associated with ARDS risk (OR = 1.41 per *HP2* allele, 95% CI [1.06, 1.88], $P = 0.018$) when
197 controlling for age, sex, ethnicity, severity of illness, plasma CFH, and presence of chronic
198 liver disease (as a surrogate for reduced hepatic Hp synthesis, **Table 2, Figure 8**). In a
199 sensitivity analysis limited to the 344 patients in whom plasma was available for measurement
200 of Hp levels, a statistically significant association between *HP* genotype and ARDS risk
201 remained (**Supplemental Table 2, Supplemental Figure 4**). Additional subgroup analyses
202 restricted to patients with detectable CFH levels ($N = 414$), Caucasian race ($N = 425$),
203 absence of chronic liver disease ($N = 469$), and patients with severe sepsis ($N = 475$) also
204 demonstrated a statistically significant association between *HP* genotype and ARDS risk (data
205 not shown).

206

207 **Haptoglobin 2 variant and ventilator-free days**

208 To assess if the *HP2* variant affected patient-centered outcomes, we tested the effect of *HP*
209 genotype on ventilator-free days (VFDs), defined as the number of days alive and not
210 receiving mechanical ventilation from ICU day 1 to ICU day 28 (40). Lower VFD values
211 indicates more prolonged mechanical ventilation, indicating more severe respiratory failure
212 (40). VFDs is a commonly reported outcome in critical care trials as it captures both duration
213 of respiratory failure as well as mortality as a competing outcome (40). Although the number
214 of VFDs decreased with each copy of *HP2*, with a mean (\pm SEM) of 15.7 (\pm 2.0) days for *HP*
215 1-1 patients; 14.0 (\pm 1.1) days for *HP* 2-1 patients; and 13.5 (\pm 1.2) days for *HP* 2-2 patients,
216 these differences were not significant ($P = 0.89$ by Kruskal-Wallis H test, **Supplemental**
217 **Figure 5**). We did not observe a difference in in-hospital mortality in ARDS patients between
218 *HP* genotypes (**Supplemental Figure 6**), nor in 28-day survival (**Supplemental Figure 7**).

219 **Discussion**

220 We have identified the *HP2* variant as a novel genetic risk factor for ARDS during sepsis. In a
221 mouse polymicrobial sepsis model, *Hp2-2* mice exposed to experimental sepsis had
222 increased lung inflammation, pulmonary vascular injury, and mortality compared with *Hp1-1*
223 mice. In a cohort of septic critically ill adults, the *HP2* variant was independently associated
224 with increased ARDS susceptibility. Moreover, the *HP2* variant was only associated with
225 increased risk of ARDS in patients with elevated plasma CFH, supporting a mechanistic role
226 for the CFH-Hp axis in ARDS pathogenesis during sepsis. These findings have significant
227 clinical implications as the *HP2* variant is more common than *HP1* in many populations of
228 European, African, South Asian, and East Asian ancestry (27), potentially affecting over
229 100,000 ARDS patients per year in the United States alone (1–3).

230

231 Endothelial injury with increased microvascular permeability is a defining pathogenic feature
232 of sepsis that leads to shock, organ failure, and death both in human studies and animal
233 models (41–48). Endothelial injury is also a key pathophysiologic characteristic of ARDS (49,
234 50). By comparing *Hp2-2* mice to *Hp1-1* mice during experimental sepsis, we found that the
235 *HP2* variant was associated with increased lung microvascular injury and increased disruption
236 of the alveolar-capillary barrier, in part due to increased apoptosis. The mechanistic impact of
237 *HP2* on ARDS during sepsis may be explained by the reduced ability of the *HP2* gene product
238 to limit the injurious effects of CFH.

239

240 The *HP2* variant is a partial copy number variant of *HP1* and contains two additional exons,
241 one of which encodes a second multimerization domain (36, 51). In humans, Hp from

242 individuals with the *HP1-1* genotype circulates in plasma as a dimer, whereas Hp from
243 individuals with *HP2-1* and *HP2-2* genotypes aggregates into progressively larger multimers
244 (27, 28, 36, 52, 53). The larger Hp2-2 multimers have reduced ability to prevent CFH-
245 mediated lipid peroxidation compared with Hp1-1 dimers, despite similar binding capacities
246 for CFH (25, 29). CFH-Hp2-2 complexes are also cleared more slowly from the extracellular
247 space by CD163 compared to CFH-Hp1-1 complexes (54), despite a greater binding affinity
248 for the CD163 receptor (23, 54). Release of CFH into the circulation during hemolysis
249 represents a significant source of oxidative stress due to the chemical reactivity of the heme
250 iron moiety. Heme-complexed iron can be oxidized from the ferrous (Fe^{2+}) state to the more
251 reactive ferric (Fe^{3+}) and ferryl (Fe^{4+}) states when outside of the reducing environment of the
252 RBC cytoplasm (21). Therefore, because Hp2-2 may have less capacity to regulate CFH-
253 mediated oxidative stress, experimental mice with *Hp2* may have increased susceptibility to
254 end-organ injury when plasma CFH levels are elevated during sepsis (15, 55).

255

256 We tested the clinical relevance of our experimental findings in a large prospective
257 observational cohort of critically ill septic adults. The *HP2* variant independently associated
258 with increased ARDS susceptibility, with an odds ratio for ARDS of 1.41 per *HP2* allele after
259 controlling for clinical factors and plasma CFH. Furthermore, *HP* genotype affected ARDS
260 susceptibility only in the subgroup of patients with elevated plasma CFH. This finding extends
261 our prior observation that higher CFH levels are associated with increased risk of organ
262 dysfunction and death during sepsis (15). In addition, our findings support the hypothesis that
263 *HP* genotype and the CFH-Hp axis have a mechanistic role in the pathogenesis of ARDS
264 during sepsis, as observed in our experimental animal model studies. Other investigators
265 have reported associations between *HP2-2* genotype and increased risk of many chronic

266 diseases such as atherosclerotic coronary artery disease (30, 31), type II diabetes (56), and
267 diabetic nephropathy (32, 33). Our current study identifies a novel clinical effect of *HP2*
268 affecting risk for a common acute clinical illness with high mortality.

269

270 The association between the *HP2* variant and increased risk of ARDS may be leveraged in
271 several ways to inform ongoing clinical and experimental research in ARDS. Genotyping the
272 *HP2* variant in patients with sepsis may be useful for risk-stratification, to identify specific
273 subpopulations at increased risk for ARDS. It may also have use in clinical trial enrichment, as
274 patients with the *HP2* variant may be more likely to benefit from pharmacological agents that
275 target the CFH-Hp axis. Furthermore, these findings may affect studies using human Hp as a
276 therapeutic agent. Human plasma-derived Hp is approved in Japan for the treatment of
277 severe hemolysis during extracorporeal cardiopulmonary bypass, severe burn injuries, or
278 massive transfusion following trauma (57–61), but this product is not approved in the United
279 States. Additional experimental studies have reported that Hp reduces CFH-induced
280 vasoconstriction, hemoglobinuria, and renal dysfunction following massive transfusion (18,
281 62, 63); cardiotoxicity following lipopolysaccharide and CFH administration (64); and organ
282 dysfunction following experimental *Staphylococcus aureus* pneumonia with massive
283 exchange transfusion (65). These experimental studies used either mixed pooled human Hp
284 (18, 62) or specifically *HP2-1* and *HP2-2* human Hp (63–65), and the clinical trials used
285 commercial pooled human Hp derived from populations with a high prevalence of *HP2-1* and
286 *HP2-2* genotypes (27, 57–61). Our current study demonstrated differential effects of *HP2-2*
287 and *HP1-1* genotypes during both experimental murine polymicrobial sepsis and in septic
288 critically ill humans. Therefore future studies using human Hp as a novel therapeutic agent
289 may need to consider the Hp phenotype in their study design to maximize clinical benefit.

290

291 Our study has several strengths. We used transgenic mice that expressed either the wild-type
292 *Hp1* or an engineered murine *Hp2* variant homologous to the human *HP2* variant (66, 67).

293 This novel murine *Hp2* variant has the same size and function as human *HP2* (66), thus
294 making it a good model to study the functional effects of *HP* genotype. *Hp2-2* mice exhibit
295 many of the same phenotypes as humans with *HP2-2* genotype including increased coronary
296 atherosclerosis (66) and increased cerebral vasospasm after subarachnoid hemorrhage (68).

297 Given the strong differences we have observed between *Hp2-2* and *Hp1-1* mice in response
298 to intraperitoneal sepsis, we propose that this model is ideal to study the molecular
299 mechanisms of the CFH-Hp axis in sepsis. Our human cohort study draws from a large well-
300 phenotyped cohort of critically ill adults hospitalized with sepsis. All clinical data were
301 collected prospectively (69). The study was sufficiently sized to determine that the association
302 between the *HP2* variant and ARDS risk was not simply due to higher severity of illness or
303 other clinical confounders. Furthermore, the size of the cohort allowed us to test the
304 association between the *HP2* variant and ARDS risk by subgroups of patients both with and
305 without detectable plasma CFH, providing further support that CFH mediates the pulmonary
306 effects of the *HP2* variant during sepsis.

307

308 Although our study advances understanding of the roles of Hp and plasma CFH in the
309 pathogenesis of ARDS, there are some limitations. We do not yet fully understand the
310 mechanisms through which CFH contributes to risk of ARDS. While the TUNEL staining
311 suggests a role for CFH-induced apoptosis, this assay is nonspecific and can also indicate
312 other forms of cell death such as necroptosis or necrosis (70). Our data suggesting
313 endothelial apoptosis is supported by previous reports showing increased apoptosis of

314 pulmonary microvascular endothelial cells in other murine sepsis models as assessed by
315 caspase activation or flow cytometry (48). We did not examine the role of CD163 in our
316 experimental sepsis model. CD163 is the primary receptor for monocyte-mediated
317 endocytosis of CFH-Hp complexes (23). Hp2-2 has different binding affinity and clearance
318 kinetics via CD163 compared with Hp1-1 (23, 54). Therefore, differential clearance of CFH-Hp
319 complexes from the circulation may also contribute to the observed differences in our model
320 between *Hp1-1* and *Hp2-2* mice. We also did not examine the role of nitric oxide (NO) in our
321 experimental sepsis model. CFH consumes NO leading to peripheral vasoconstriction in
322 patients with sickle cell anemia (71), and NO depletion is a common feature of both chronic
323 pulmonary vascular disease (72) and red blood cell transfusion (17), a known etiology of
324 ARDS (55, 73). Hp binding does not appear to attenuate CFH-mediated NO scavenging (62,
325 74), however the slower clearance kinetics of CFH-Hp2-2 complex (54, 74) could also affect
326 the rate of NO depletion in the pulmonary vascular endothelium of *HP2-2* individuals during
327 sepsis. The cellular mechanisms by which CFH causes disruption of the pulmonary vascular
328 endothelial barrier will require further study. We identified sepsis using the “Sepsis-2”
329 definition (75) as all study patients were enrolled prior to the publication of the more recent
330 Third International Consensus definition of sepsis (76). Since we enrolled patients exclusively
331 from ICUs, the overwhelming majority ($N = 475$, 95.7%) of sepsis patients in our cohort also
332 had “severe sepsis” (defined as sepsis with concomitant organ dysfunction or hypoperfusion),
333 which is analogous to the more recent “Sepsis-3” definition (76). We found similar results
334 when limiting our analyses to patients with severe sepsis. Lastly, although we noted a high
335 correlation between imputed *HP* genotype and PCR *HP* genotype in our human study without
336 any evidence of systematic bias, we cannot exclude the possibility of some misclassification
337 among imputed genotypes, particularly between *HP2-1* and *HP2-2*. Reassuringly, we did not

338 observe any misclassification in patients predicted to have *HP1-1* by imputation, although the
339 sample size of this group was relatively small.

340

341 In summary, we have demonstrated for the first time that the *HP2* variant represents a novel
342 genetic risk factor for ARDS susceptibility during sepsis. In an experimental polymicrobial
343 sepsis model, *Hp2-2* mice had increased lung inflammation, pulmonary microvascular
344 permeability, lung apoptosis, and death. In critically ill patients with sepsis, each additional
345 *HP2* allele was associated with an increased risk of ARDS, independent of potential
346 confounders. These findings have important clinical implications as *HP2* is the more common
347 variant in many human populations. This study identifies a large clinical sub-population of
348 sepsis patients who are genetically predisposed to develop ARDS, and has important
349 implications for further research into the role of the CFH-Hp axis during critical illness.

350 **Methods**

351 **Transgenic murine model of polymicrobial sepsis**

352 Transgenic mice with murine homologues of human *Hp1-1* and *Hp2-2* were a kind gift from
353 Dr. Rafael Tamargo of the Johns Hopkins University School of Medicine (67). We used a
354 previously reported murine model of polymicrobial sepsis (77, 78). We prepared a cecal slurry
355 (CS) from six-week-old female C57BL/6 donor mice purchased from The Jackson Laboratory
356 (Bar Harbor, ME). In brief, cecal contents were collected from euthanized donor mice,
357 resuspended in 5% dextrose at 80 mg/mL, vortexed for fifteen seconds, and filtered through a
358 25 gauge needle. We administered an intraperitoneal injection CS at 2.0 mg / gram body
359 weight (BW) and a retro-orbital injection of CFH at 0.15 mg / gram BW to recipient 8-12-week-
360 old male and female transgenic mice as previously reported (79). The CFH injection was
361 included to increase plasma CFH levels to levels observed in human sepsis (79). We
362 monitored the study mice for 72 hours during survival studies. Mice were monitored closely
363 for signs of pain following induction of experimental sepsis. Antibiotics were not administered
364 in this model of sepsis to allow robust bacterial growth and dissemination, which better
365 reflects the natural history of sepsis in patients before seeking medical care. For all other
366 studies, we euthanized the study mice with pentobarbital at four or twenty-four hours after CS
367 administration for collection of samples. The Vanderbilt Institutional Animal Care and Use
368 Committee approved all animal experiments.

369

370 **Mouse sample collection**

371 Blood was collected by retro-orbital puncture in heparinized syringes and centrifuged at
372 2,000x g for ten minutes. Bronchoalveolar lavage fluid was collected as previously described

373 (80), as were excised whole lungs which were immediately flash frozen in liquid nitrogen. We
374 stored all samples at -80 °C until time of analysis.

375

376 **Plasma circulating cell-free hemoglobin in mice**

377 Plasma CFH was measured at twenty-four hours in mouse plasma using the HemoCue®
378 Plasma/Low Hb System (HemoCue America, Brea, CA).

379

380 **Lung inflammation biomarkers in mice**

381 We measured chemokine ligand 1 (CXCL1/KC) in duplicate using an
382 electrochemiluminescence assay (MesoScale Discovery, Gaithersburg, MD) in BAL samples
383 according to the manufacturer's recommendations. For mRNA expression, we extracted
384 mRNA from flash frozen whole lungs using Qiagen RNeasy Plus Mini Kit (Hilden, Germany).
385 We generated cDNA using a SuperScript VILO cDNA Synthesis Kit (Invitrogen, Carlsbad,
386 CA), and quantified CXCL1 mRNA expression level by quantitative PCR, normalized to
387 GAPDH expression using TaqMan® primer probes (Thermo Fisher Scientific, Waltham, MA).

388

389 **Myeloperoxidase activity**

390 Frozen lungs were homogenized frozen in 50 mM potassium phosphate (pH 6.0), 0.5%
391 hexadecyltrimethylammonium bromide, and 5mM EDTA, then sonicated, centrifuged, and
392 diluted at 1:30 dilution in 100 mM potassium phosphate (pH 6.0), 0.3% hydrogen peroxide
393 (Sigma-Aldrich, St Louis, MO), and 1 mg/ml *o*-dianisidine (Sigma-Aldrich). We recorded
394 absorbance at 460 nm using a spectrophotometer at one and three minutes, and calculated
395 MPO activity according to the equation (81):

396 Activity = $[A_{460\text{ nm}, 1\text{ min}} - A_{460\text{ nm}, 3\text{ min}}] \times 13.5 / \text{weight}_{\text{lung}}$

397

398 **Lung apoptosis**

399 At the time of organ harvest, we perfused lungs with 10% formalin. Cell apoptosis was
400 ascertained using the Fluorescein In Situ Cell Death Detection Kit (Roche, Basel,
401 Switzerland) on paraffin fixed sections of mouse lung following deparaffinization and antigen
402 retrieval. A trained reviewer who was blinded to each sample's *Hp* genotype examined lung
403 histology slides and identified the number of cells undergoing apoptosis per low power field.
404 Using endothelial co-labeling in samples from wild type mice, we have previously determined
405 that 80% of apoptotic lung cells in this model are endothelial (Bastarache JA, et al.,
406 unpublished observations).

407

408 **Pulmonary vascular permeability by AngioSense assay**

409 In selected experiments, we administered 100 μl AngioSense[®] 750EX near-infrared
410 fluorescent imaging agent (2 nmol/ 100 μl) to each study mouse via retro-orbital injection. We
411 measured extravascular accumulation of the imaging agent of excised lungs at twenty-four
412 hours using a LI-COR Pearl[®] small-animal imaging camera (LI-COR Biosciences, Lincoln,
413 NE).

414

415 **Human study population and clinical data collection**

416 We studied patients ≥ 18 years of age enrolled in the Validating Acute Lung Injury markers for
417 Diagnosis (VALID) study, a prospective observational cohort study of critically ill patients at
418 high risk for ARDS and other acute organ dysfunction (69). We included patients with sepsis

419 on admission to the ICU as defined by the ACCP/SCCM Consensus (“Sepsis-2”) Criteria (75)
420 with plasma samples available for CFH measurement and DNA samples available for
421 genotyping. Sepsis was defined using the Sepsis-2 criteria because all patients included in
422 the study were enrolled prior to the publication of the Third International Consensus definition
423 of sepsis (76). Study personnel collected clinical data including medications, vital signs,
424 laboratory studies, severity of illness scores, organ failures by the Brussels criteria (37), and
425 chest radiographs for ARDS phenotyping (82) for the 24 hours prior to enrollment and daily for
426 the first four days after enrollment.

427

428 **Human samples collection and assays**

429 Study personnel collected blood samples on the morning of ICU day 2 at the time of
430 enrollment, and preferentially drew blood through a central venous catheter to minimize
431 hemolysis. We measured CFH (HemoCue[®] Plasma/Low Hb System, HemoCue America,
432 Brea, CA) and haptoglobin (Abcam[®]) in plasma as previously described (15). There was
433 insufficient plasma available to measure haptoglobin levels in 152 patients. We have
434 previously reported some of the hemoglobin and haptoglobin levels (15, 83). We extracted
435 genomic DNA from buffy coat peripheral blood leukocytes using Gentra PureGene blood kit
436 (Qiagen) according to manufacturer protocols and stored at -80C until genotyping.

437

438 **Haptoglobin genotyping**

439 We genotyped *HP* by measuring the ratio of *HP5'* (a region common to both the *HP1* and
440 *HP2* variants) to *HP2* (a region specific to *HP2* variant) via TaqMan[®] based real time
441 polymerase chain reaction (RT-PCR) as previously described (84). We calculated the change

442 in threshold cycle (ΔC_t) for each sample as $C_{t_{HP5'}} - C_{t_{HP2}}$, and calculated the HP2/HP5' ratio of
443 each sample as $2^{-\Delta C_t \text{ sample}}$. We defined *HP1-1* by a HP2/HP5' ratio of zero, *HP2-1* by a ratio
444 between 0 and 0.60, and *HP2-2* by a ratio above 0.60. We confirmed the accuracy of our
445 PCR genotyping method in a subset of samples with gel electrophoresis to determine
446 haptoglobin phenotype (85) using study personnel blinded to the PCR genotyping results.

447

448 **Haptoglobin genotype imputation**

449 In 152 Caucasian patients, we imputed *HP* genotype from genome-wide microarray data.
450 Genotyping was performed at the W.M. Keck facility at Yale University as part of previously
451 reported genome-wide association study of acute kidney injury (86) using the Illumina
452 HumanOmni1 Quad v1.0 BeadChip. We used the genotyping v1.9.4 module clustering
453 algorithm from Illumina GenomeStudio™ software for SNP calling (Illumina, San Diego, CA).
454 Patients with sample genotype call rate under 97% and patients with a discrepancy between
455 X-chromosome zygosity and reported sex were excluded (86). We extracted SNPs within a 2
456 megabase region surrounding the *HP* gene (Hg19 chr16:71,036,975-73,063,764), then
457 phased the target region and imputed *HP* genotype using the Beagle version 3.3.2 algorithm
458 (87) with a phased reference panel provided by Boettger et al. (36). The reference panel
459 consisted of 274 unrelated individuals of European ancestry from the 1000 Genomes Project
460 (88) and HapMap3 project (89) who underwent genotyping on several GWAS platforms as
461 well as droplet-digital PCR *HP* genotyping (36). We used the default parameters for Beagle
462 with fifty iterations of the phasing algorithm and twenty-five haplotypes sampled for each
463 individual during each iteration. We used the calculated genotype posterior-probabilities for
464 number of *HP2* alleles as the surrogate for *HP* genotype, with a *HP2* genotype probability of

465 0.0 to 0.5 corresponding to a predicted *HP* genotype of *HP1-1*, a genotype probability of 0.5
466 to 1.5 corresponding to *HP2-1*, and a genotype probability of 1.5 to 2.0 corresponding to
467 *HP2-2*.

468

469 **Statistical analysis for experimental mouse studies**

470 For the survival study using the experimental sepsis model, we estimated the survival function
471 using the method of Kaplan and Meier and assessed differences in survival using the Mantel-
472 Cox log rank test. For all biomarker studies, data are presented as the median \pm IQR. We
473 used the Mann-Whitney-U test for comparisons of continuous variables between *Hp1-1* and
474 *Hp2-2* mice.

475

476 **Statistical analysis for human studies**

477 The primary outcome of the human study was prevalence of ARDS defined by the Berlin
478 Criteria (82) on at least one of the first four ICU study days. We performed a secondary
479 analysis focused on patients with detectable plasma CFH levels defined as ≥ 10 mg/dL to test
480 the hypothesis that the effect of *HP* genotype is magnified when plasma CFH levels are
481 elevated. Differences in genotype distributions were tested using the Binomial proportion test
482 for observed *HP2* allele frequencies. We used the Cochran-Armitage Test for trend to test
483 categorical outcomes versus CFH quartiles and *HP* genotype, using the alternative
484 hypothesis that risk increases with each *HP2* allele. Differences in continuous outcomes
485 between *HP* genotypes was tested using one-way ANOVA for variables with normal
486 distributions and the Kruskal-Wallis *H* test for variables with non-normal distributions. We also
487 tested the association between *HP* genotype and ARDS using multivariable logistic regression

488 to control for potential clinical and biochemical confounders including age, sex, ethnicity,
489 severity of illness (by APACHE II score) (90), plasma CFH levels, and presence of chronic
490 liver disease as a surrogate for hepatic haptoglobin synthetic function. We calculated number
491 of ventilator-free days (VFDs) during the first 28 days using an accepted definition (40): 0 if
492 the patient died during the first 28 days following enrollment in the study, or $28 - x$ if the
493 patient was successfully weaned from mechanical ventilation, where x was the number of
494 days receiving mechanical ventilation after enrollment in the study. Categorical outcomes are
495 presented as percentage (number with outcome). Continuous outcomes are presented as
496 mean \pm SEM for outcomes with normal distributions and for VFDs (40), and median \pm IQR for
497 all other non-normally distributed outcomes. A P value of less than 0.05 was considered
498 significant.

499

500 To assess the accuracy of imputation-based *HP* genotyping, we compared imputed *HP*
501 genotype with PCR-determined *HP* genotype as the gold-standard in 120 patients with data
502 available for both methods. We constructed a 3x3 confusion matrix and calculated sensitivity,
503 specificity, and F-statistics for all three possible imputed genotypes. We also calculated
504 overall accuracy and unweighted Cohen's kappa correlation statistic. We used R version 3.5.1
505 (91) using the packages DescTools (92) and rms (93) for statistical testing and RStudio
506 version 1.0.147 (94) with the package ggplot2 (95) for data visualization.

507

508 **Study Approval**

509 The Vanderbilt University Medical Center Institutional Animal Care and Use Committee
510 (Nashville, TN) reviewed and approved all animal study protocols. The Vanderbilt University

511 Medical Center Institutional Review Board (Nashville, TN) reviewed and approved the VALID
512 study protocol (IRB #051065). Study personnel obtained informed consent from the patient or
513 the patient's surrogate decision maker whenever possible. The IRB approved a waiver of
514 consent when the patient could not give consent due to severity of medical illness and no
515 surrogate decision-maker was available.

515 **Author Contributions**

516 VEK, JAB, CMS, and LBW designed the study, provided data analysis and figure generation,
517 performed statistical analyses, and wrote / edited the manuscript. VEK designed and
518 implemented computer scripts for haptoglobin imputation. HN, JBN, SRL, NDP, WKU, JJ,
519 NEW, TNS, and DRJ performed relevant experiments. LBW, CRP, and EDS provided genetic
520 microarray data and performed quality control. All authors reviewed and approved the final
521 version of the manuscript.

522 **Acknowledgements**

523 This work is supported by NIH T32 GM108554 and NLM T15 LM007450 (VEK), NIH HL
524 135849 (LBW and JAB), NIH HL 103836 (LBW), NIH HL 136888 (CMS), Parker B. Francis
525 Foundation (CMS), Vanderbilt Faculty Research Scholars (CMS). The project publication
526 described was supported by CTSA award No. UL1 TR002243 from the National Center for
527 Advancing Translational Sciences. Its contents are solely the responsibility of the authors and
528 do not necessarily represent official views of the National Center for Advancing Translational
529 Sciences or the National Institutes of Health. The authors would like to acknowledge Linda
530 Boettger and Steven Carroll of the Broad Institute of MIT and Harvard for kindly providing the
531 reference panels for haptoglobin imputation and their advice on implementation, Neil Zheng
532 for assistance with implementation of haptoglobin imputation, and Dr. Rafael Tamargo of the
533 Department of Neurosurgery at the Johns Hopkins University School of Medicine for providing
534 the transgenic mice used in this study.

1. Rubenfeld GD et al. Incidence and Outcomes of Acute Lung Injury. *N. Engl. J. Med.* 2005;353(16):1685–1693.
2. Rubenfeld GD, Herridge MS. Epidemiology and Outcomes of Acute Lung Injury. *Chest* 2007;131(2):554–562.
3. Eworuke E, Major JM, Gilbert McClain LI. National incidence rates for Acute Respiratory Distress Syndrome (ARDS) and ARDS cause-specific factors in the United States (2006–2014). *J. Crit. Care* 2018;47:192–197.
4. Thompson BT, Chambers RC, Liu KD. Acute Respiratory Distress Syndrome. *N. Engl. J. Med.* 2017;377(6):562–572.
5. Bosma KJ, Taneja R, Lewis JF. Pharmacotherapy for Prevention and Treatment of Acute Respiratory Distress Syndrome. *Drugs* 2010;70(10):1255–1282.
6. Fan E, Brodie D, Slutsky AS. Acute Respiratory Distress Syndrome: Advances in Diagnosis and Treatment. *JAMA* 2018;319(7):698–710.
7. Bellani G et al. Epidemiology, Patterns of Care, and Mortality for Patients With Acute Respiratory Distress Syndrome in Intensive Care Units in 50 Countries. *JAMA* 2016;315(8):788–800.
8. Meyer NJ, Christie JD. Genetic Heterogeneity and Risk of Acute Respiratory Distress Syndrome. *Semin. Respir. Crit. Care Med.* 2013;34(4):459–474.
9. Pham T, Rubenfeld GD. Fifty Years of Research in ARDS. The Epidemiology of Acute Respiratory Distress Syndrome. A 50th Birthday Review. *Am. J. Respir. Crit. Care Med.* 2017;195(7):860–870.

10. Doyle RL, Szaflarski N, Modin GW, Wiener-Kronish JP, Matthay MA. Identification of patients with acute lung injury. Predictors of mortality.. *Am. J. Respir. Crit. Care Med.* 1995;152(6):1818–1824.
11. Machiedo GW, Powell RJ, Rush BF, Swislocki NI, Dikdan G. The Incidence of Decreased Red Blood Cell Deformability in Sepsis and the Association With Oxygen Free Radical Damage and Multiple-System Organ Failure. *Arch. Surg.* 1989;124(12):1386–1389.
12. Baskurt OK, Gelmont D, Meiselman HJ. Red Blood Cell Deformability in Sepsis. *Am. J. Respir. Crit. Care Med.* 1998;157(2):421–427.
13. Piagnerelli M, Boudjeltia KZ, Vanhaeverbeek M, Vincent J-L. Red blood cell rheology in sepsis. *Intensive Care Med.* 2003;29(7):1052–1061.
14. Kempe DS et al. Suicidal erythrocyte death in sepsis. *J. Mol. Med.* 2007;85(3):273–281.
15. Janz DR et al. Association Between Cell-Free Hemoglobin, Acetaminophen, and Mortality in Patients With Sepsis: An Observational Study. *Crit. Care Med.* 2013;41(3):784–790.
16. Adamzik M et al. Free hemoglobin concentration in severe sepsis: methods of measurement and prediction of outcome. *Crit. Care* 2012;16(4):R125.
17. Donadee C et al. Nitric Oxide Scavenging by Red Blood Cell Microparticles and Cell-Free Hemoglobin as a Mechanism for the Red Cell Storage Lesion. *Circulation* 2011;124(4):465–476.
18. Baek JH et al. Hemoglobin-driven pathophysiology is an in vivo consequence of the red blood cell storage lesion that can be attenuated in guinea pigs by haptoglobin therapy. *J. Clin. Invest.* 2012;122(4):1444–1458.

19. Graça-Souza AV, Arruda MAB, Freitas MS de, Barja-Fidalgo C, Oliveira PL. Neutrophil activation by heme: implications for inflammatory processes. *Blood* 2002;99(11):4160–4165.
20. Billings FT, Ball SK, Roberts LJ, Pretorius M. Postoperative Acute Kidney Injury is Associated with Hemoglobinemia and an Enhanced Oxidative Stress Response. *Free Radic. Biol. Med.* 2011;50(11):1480–1487.
21. Reeder BJ, Svistunenko DA, Cooper CE, Wilson MT. The Radical and Redox Chemistry of Myoglobin and Hemoglobin: From In Vitro Studies to Human Pathology. *Antioxid. Redox Signal.* 2004;6(6):954–966.
22. Wicher KB, Fries E. Haptoglobin, a hemoglobin-binding plasma protein, is present in bony fish and mammals but not in frog and chicken. *Proc. Natl. Acad. Sci.* 2006;103(11):4168–4173.
23. Kristiansen M et al. Identification of the haemoglobin scavenger receptor. *Nature* 2001;409(6817):198–201.
24. Schaer DJ, Buehler PW, Alayash AI, Belcher JD, Vercellotti GM. Hemolysis and free hemoglobin revisited: exploring hemoglobin and hemin scavengers as a novel class of therapeutic proteins. *Blood* 2013;121(8):1276–1284.
25. Gutteridge JMC. The antioxidant activity of haptoglobin towards haemoglobin-stimulated lipid peroxidation. *Biochim. Biophys. Acta Lipids Lipid Metab.* 1987;917(2):219–223.
26. Maeda N, Smithies O. The evolution of multigene families: human haptoglobin genes. *Annu. Rev. Genet.* 1986;20(1):81–108.
27. Carter K, Worwood M. Haptoglobin: a review of the major allele frequencies worldwide and their association with diseases. *Int. J. Lab. Hematol.* 2007;29(2):92–110.

28. Okazaki T, Yanagisawa Y, Nagai T. Analysis of the affinity of each haptoglobin polymer for hemoglobin by two-dimensional affinity electrophoresis. *Clin. Chim. Acta* 1997;258(2):137–144.
29. Melamed-Frank M et al. Structure-function analysis of the antioxidant properties of haptoglobin. *Blood* 2001;98(13):3693–3698.
30. Levy AP et al. Haptoglobin phenotype is an independent risk factor for cardiovascular disease in individuals with diabetes: the strong heart study. *J. Am. Coll. Cardiol.* 2002;40(11):1984–1990.
31. Roguin A et al. Haptoglobin Genotype Is Predictive of Major Adverse Cardiac Events in the 1-Year Period After Percutaneous Transluminal Coronary Angioplasty in Individuals With Diabetes. *Diabetes Care* 2003;26(9):2628–2631.
32. Nakhoul FM et al. Haptoglobin phenotype and diabetic nephropathy. *Diabetologia* 2001;44(5):602–604.
33. Orchard TJ et al. Haptoglobin Genotype and the Rate of Renal Function Decline in the Diabetes Control and Complications Trial/Epidemiology of Diabetes Interventions and Complications Study. *Diabetes* 2013;62(9):3218–3223.
34. Ohnishi H et al. Haptoglobin Phenotype Predicts Cerebral Vasospasm and Clinical Deterioration after Aneurysmal Subarachnoid Hemorrhage. *J. Stroke Cerebrovasc. Dis.* 2013;22(4):520–526.
35. Kantor E et al. Haptoglobin genotype and functional outcome after aneurysmal subarachnoid hemorrhage. *J. Neurosurg.* 2014;120(2):386–390.
36. Boettger LM et al. Recurring exon deletions in the HP (haptoglobin) gene contribute to lower blood cholesterol levels. *Nat. Genet.* 2016;48(4):359-366A.

37. Bernard G. The Brussels Score. *Sepsis* 1997;1(1):43–44.
38. Kasvosve I et al. Reference range of serum haptoglobin is haptoglobin phenotype-dependent in blacks. *Clin. Chim. Acta* 2000;296(1):163–170.
39. Imrie H et al. Haptoglobin levels are associated with haptoglobin genotype and α -Thalassemia in a malaria-endemic area. *Am. J. Trop. Med. Hyg.* 2006;74(6):965–971.
40. Schoenfeld DA, Bernard GR. Statistical evaluation of ventilator-free days as an efficacy measure in clinical trials of treatments for acute respiratory distress syndrome. *Crit. Care Med.* 2002;30(8):1772.
41. Lee WL, Slutsky AS. Sepsis and Endothelial Permeability. *N. Engl. J. Med.* 2010;363(7):689–691.
42. Goldenberg NM, Steinberg BE, Slutsky AS, Lee WL. Broken Barriers: A New Take on Sepsis Pathogenesis. *Sci. Transl. Med.* 2011;3(88):88ps25-88ps25.
43. Shapiro NI et al. The association of endothelial cell signaling, severity of illness, and organ dysfunction in sepsis. *Crit. Care* 2010;14(5):R182.
44. Sessler CN et al. Circulating ICAM-1 is increased in septic shock. *Am. J. Respir. Crit. Care Med.* 1995;151(5):1420–1427.
45. Mutunga M et al. Circulating Endothelial Cells in Patients with Septic Shock. *Am. J. Respir. Crit. Care Med.* 2001;163(1):195–200.
46. Shapiro NI et al. Skin Biopsies Demonstrate Site-Specific Endothelial Activation in Mouse Models of Sepsis. *J. Vasc. Res.* 2009;46(5):495–502.
47. London NR et al. Targeting Robo4-Dependent Slit Signaling to Survive the Cytokine Storm in Sepsis and Influenza. *Sci. Transl. Med.* 2010;2(23):23ra19-23ra19.

48. Gill SE, Taneja R, Rohan M, Wang L, Mehta S. Pulmonary Microvascular Albumin Leak Is Associated with Endothelial Cell Death in Murine Sepsis-Induced Lung Injury In Vivo. *PLoS ONE* 2014;9(2). doi:10.1371/journal.pone.0088501
49. Matthay MA, Zemans RL. The Acute Respiratory Distress Syndrome: Pathogenesis and Treatment. *Annu. Rev. Pathol.* 2011;6:147–163.
50. Millar FR, Summers C, Griffiths MJ, Toshner MR, Proudfoot AG. The pulmonary endothelium in acute respiratory distress syndrome: insights and therapeutic opportunities. *Thorax* 2016;71(5):462–473.
51. Maeda N, Yang F, Barnett DR, Bowman BH, Smithies O. Duplication within the haptoglobin Hp2 gene. *Nature* 1984;309(5964):131–135.
52. Smithies O. Grouped Variations in the Occurrence of New Protein Components in Normal Human Serum. *Nature* 1955;175(4450):307.
53. Smithies O, Walker NF. Genetic Control of some Serum Proteins in Normal Humans. *Nature* 1955;176(4496):1265.
54. Asleh R et al. Genetically Determined Heterogeneity in Hemoglobin Scavenging and Susceptibility to Diabetic Cardiovascular Disease. *Circ. Res.* 2003;92(11):1193–1200.
55. Janz DR, Ware LB. The role of red blood cells and cell-free hemoglobin in the pathogenesis of ARDS. *J. Intensive Care* 2015;3:20.
56. Shi X et al. Haptoglobin 2-2 Genotype Is Associated with Increased Risk of Type 2 Diabetes Mellitus in Northern Chinese. *Genet. Test. Mol. Biomark.* 2012;16(6):563–568.
57. Japan Blood Products Organization. Human Haptoglobin General Product Information Overview [Internet]. <https://www.jbpo.or.jp/med/di/file/6451/>. Accessed December 31, 2018

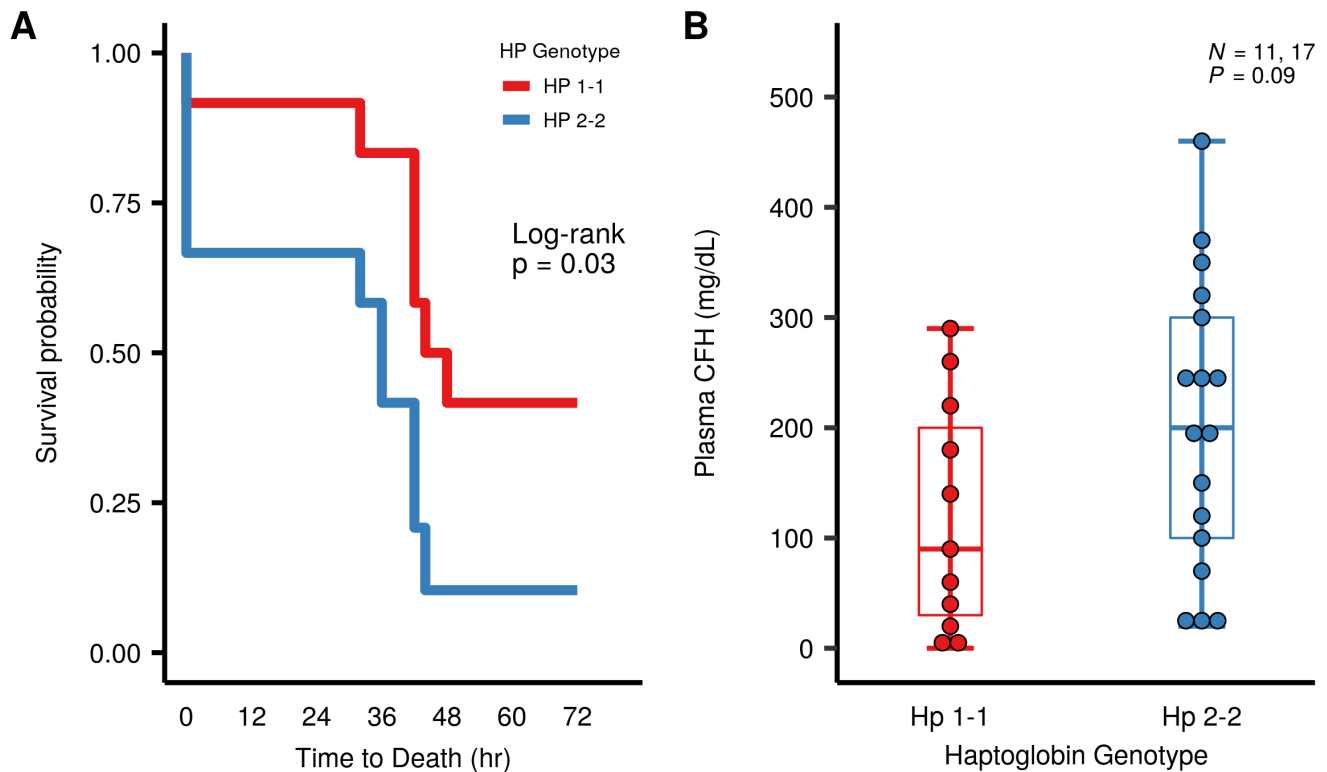
58. Yamamoto H, Kudo R, Nishikawa S, Yamazaki K. Efficacy of haptoglobin administration in the early postoperative course of patients with a diagnosis of HELLP syndrome. *J. Obstet. Gynaecol.* 2000;20(6):610–611.
59. Hashimoto K, Nomura K, Nakano M, Sasaki T, Kurosawa H. Pharmacological intervention for renal protection during cardiopulmonary bypass. *Heart Vessels* 1993;8(4):203–210.
60. Kanamori Y et al. The effects of administration of haptoglobin for hemolysis by extracorporeal circulation. [in Japanese]. *Rinsho Kyobu Geka* 1989;9(5):463–467.
61. Gando S, Tedo I. The effects of massive transfusion and haptoglobin therapy on hemolysis in trauma patients. *Surg. Today* 1994;24(9):785–790.
62. Boretti FS et al. Sequestration of extracellular hemoglobin within a haptoglobin complex decreases its hypertensive and oxidative effects in dogs and guinea pigs. *J. Clin. Invest.* 2009;119(8):2271–2280.
63. Graw Jan A. et al. Haptoglobin or Hemopexin Therapy Prevents Acute Adverse Effects of Resuscitation After Prolonged Storage of Red Cells. *Circulation* 2016;134(13):945–960.
64. Baek JH et al. Extracellular Hb Enhances Cardiac Toxicity in Endotoxemic Guinea Pigs: Protective Role of Haptoglobin. *Toxins* 2014;6(4):1244–1259.
65. Remy KE et al. Haptoglobin improves shock, lung injury, and survival in canine pneumonia. *JCI Insight* 2018;3(18):e123013.
66. Levy AP et al. Haptoglobin Genotype Is a Determinant of Iron, Lipid Peroxidation, and Macrophage Accumulation in the Atherosclerotic Plaque. *Arterioscler. Thromb. Vasc. Biol.* 2007;27(1):134–140.

67. Pradilla G et al. Systemic L-Citrulline Prevents Cerebral Vasospasm in Haptoglobin 2-2 Transgenic Mice After Subarachnoid Hemorrhage. *Neurosurgery* 2012;70(3):747–757.
68. Chaichana KL, Levy AP, Miller-Lotan R, Shakur S, Tamargo RJ. Haptoglobin 2-2 Genotype Determines Chronic Vasospasm After Experimental Subarachnoid Hemorrhage. *Stroke* 2007;38(12):3266–3271.
69. O’Neal HR et al. Prehospital Statin and Aspirin Use and the Prevalence of Severe Sepsis and ALI/ARDS. *Crit. Care Med.* 2011;39(6):1343–1350.
70. Kelly KJ, Sandoval RM, Dunn KW, Molitoris BA, Dagher PC. A novel method to determine specificity and sensitivity of the TUNEL reaction in the quantitation of apoptosis. *Am. J. Physiol. Cell Physiol.* 2003;284(5):C1309–C1318.
71. Reiter CD et al. Cell-free hemoglobin limits nitric oxide bioavailability in sickle-cell disease. *Nat. Med.* 2002;8(12):1383–1389.
72. Brittain EL et al. Elevation of Plasma Cell-Free Hemoglobin in Pulmonary Arterial Hypertension. *Chest* 2014;146(6):1478–1485.
73. Janz DR et al. Longer storage duration of red blood cells is associated with an increased risk of acute lung injury in patients with sepsis. *Ann. Intensive Care* 2013;3(1):33.
74. Azarov I et al. Rate of Nitric Oxide Scavenging by hemoglobin bound to haptoglobin. *Nitric Oxide.* 2008;18(4):296–302.
75. Levy MM et al. 2001 SCCM/ESICM/ACCP/ATS/SIS International Sepsis Definitions Conference. *Intensive Care Med.* 2003;29(4):530–538.
76. Singer M et al. The Third International Consensus Definitions for Sepsis and Septic Shock (Sepsis-3). *JAMA* 2016;315(8):801–810.

77. Wynn JL et al. Increased mortality and altered immunity in neonatal sepsis produced by generalized peritonitis. *Shock* 2007;28(6):675–683.
78. Wynn JL et al. Defective innate immunity predisposes murine neonates to poor sepsis outcome but is reversed by TLR agonists. *Blood* 2008;112(5):1750–1758.
79. Shaver CM et al. Cell-free hemoglobin augments acute kidney injury during experimental sepsis. *Am. J. Physiol.-Ren. Physiol.* [published online ahead of print: July 31, 2019]; doi:10.1152/ajprenal.00375.2018
80. Bastarache JA et al. Low levels of tissue factor lead to alveolar haemorrhage, potentiating murine acute lung injury and oxidative stress. *Thorax* 2012;67(12):1032–1039.
81. Blackwell TS, Lancaster LH, Blackwell TR, Venkatakrisnan A, Christman JW. Chemotactic Gradients Predict Neutrophilic Alveolitis in Endotoxin-treated Rats. *Am. J. Respir. Crit. Care Med.* 1999;159(5):1644–1652.
82. Ferguson ND et al. The Berlin definition of ARDS: an expanded rationale, justification, and supplementary material. *Intensive Care Med.* 2012;38(10):1573–1582.
83. Janz DR et al. Association between haptoglobin, hemopexin and mortality in adults with sepsis. *Crit. Care* 2013;17:R272.
84. Soejima M, Koda Y. TaqMan-Based Real-Time PCR for Genotyping Common Polymorphisms of Haptoglobin (HP1 and HP2). *Clin. Chem.* 2008;54(11):1908–1913.
85. Koch W et al. Genotyping of the Common Haptoglobin Hp 1/2 Polymorphism Based on PCR. *Clin. Chem.* 2002;48(9):1377–1382.
86. Zhao B et al. A Genome-Wide Association Study to Identify Single-Nucleotide Polymorphisms for Acute Kidney Injury. *Am. J. Respir. Crit. Care Med.* 2017;195(4):482–490.

87. Browning SR, Browning BL. Rapid and Accurate Haplotype Phasing and Missing-Data Inference for Whole-Genome Association Studies By Use of Localized Haplotype Clustering. *Am. J. Hum. Genet.* 2007;81(5):1084–1097.
88. The 1000 Genomes Project Consortium. A global reference for human genetic variation. *Nature* 2015;526(7571):68–74.
89. The International HapMap Consortium, Altshuler D, Donnelly P. A haplotype map of the human genome. *Nature* 2005;437(7063):1299–1320.
90. Knaus WA, Draper EA, Wagner DP, Zimmerman JE. APACHE II: a severity of disease classification system. *Crit. Care Med.* 1985;13(10):818–829.
91. R Core Team. *R: A Language and Environment for Statistical Computing*. Vienna, Austria: R Foundation for Statistical Computing; 2017.
92. Signorell A. *DescTools: Tools for Descriptive Statistics* [computer program]. 2018.
93. Harell Jr. FE. *rms: Regression Modeling Strategies* [computer program]. 2018.
94. RStudio Team. *RStudio: Integrated Development Environment for R* [computer program]. Boston, MA: RStudio, Inc.; 2016.
95. Wickham H. *ggplot2: Elegant Graphics for Data Analysis* [computer program]. Springer-Verlag, New York; 2016.

537 **Figures**

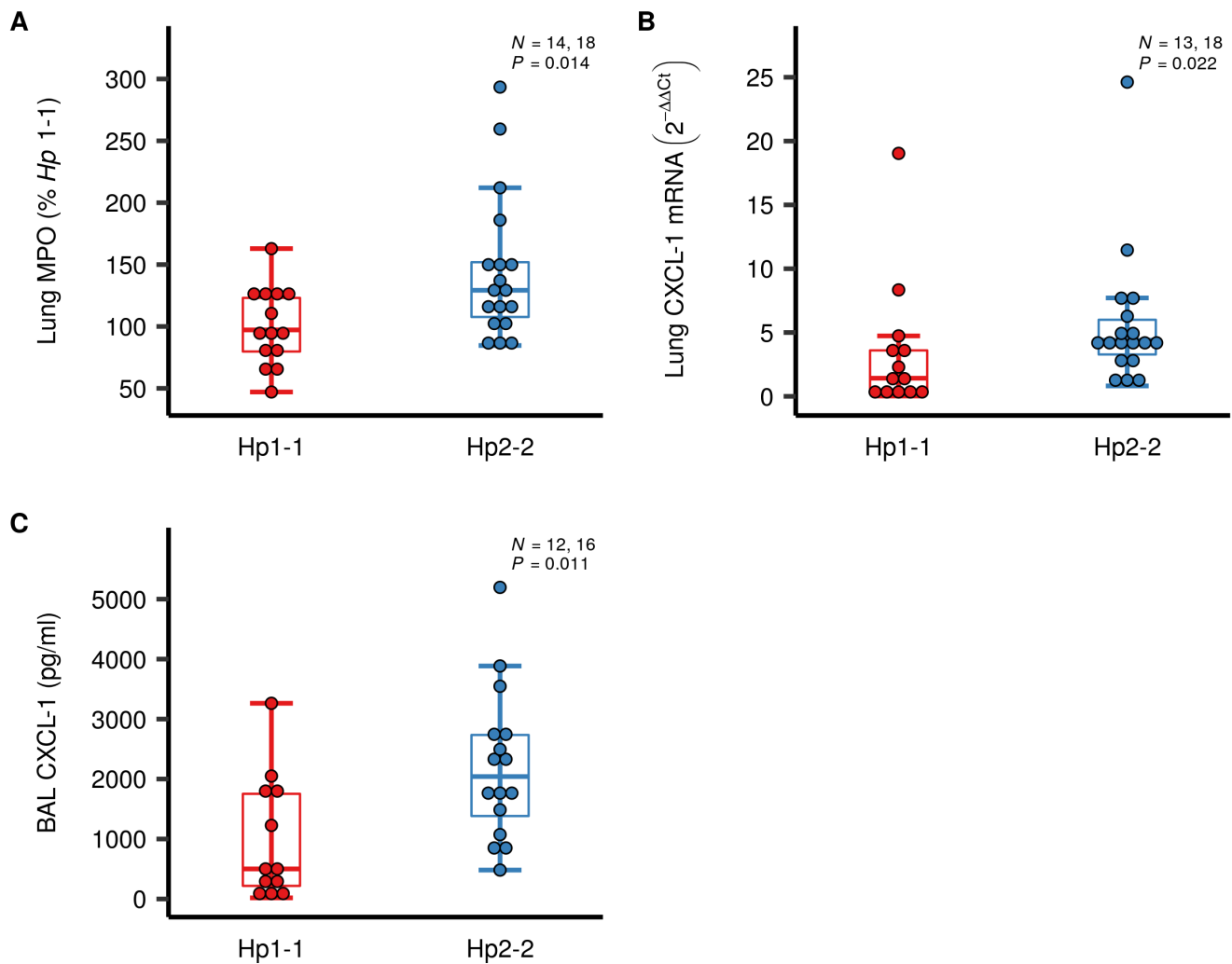


538

539 **Figure 1. *Hp2-2* mice have decreased survival over 72 hours following experimental**
540 **sepsis**

541 *Hp1-1* (red) and *Hp2-2* (blue) mice ($n = 12$ each group) were treated with intraperitoneal
542 injection of 2.0 mg cecal slurry per gram body weight and intravenous injection of 100 μ l of
543 0.15 mg/mL CFH, then monitored for survival over 72 hours. (A) Survival curves showing
544 survival was significantly worse in *Hp2-2* mice. * $P = 0.03$ by the Mantel-Cox log rank test. (B)
545 Plasma CFH levels were measured at 24 hours in *Hp1-1* ($n = 11$) and *Hp2-2* ($n = 17$) mice
546 treated with CS and IV CFH. Dots represent individual values. In the box plots, the thick
547 horizontal bars represent the median, boxes represent the interquartile range (IQR, 25th and

548 75th percentiles), and whiskers represent the minimum and maximum values within $1.5 * IQR$
549 from the 25th and 75th percentiles. $P = 0.09$ by Mann-Whitney U test.

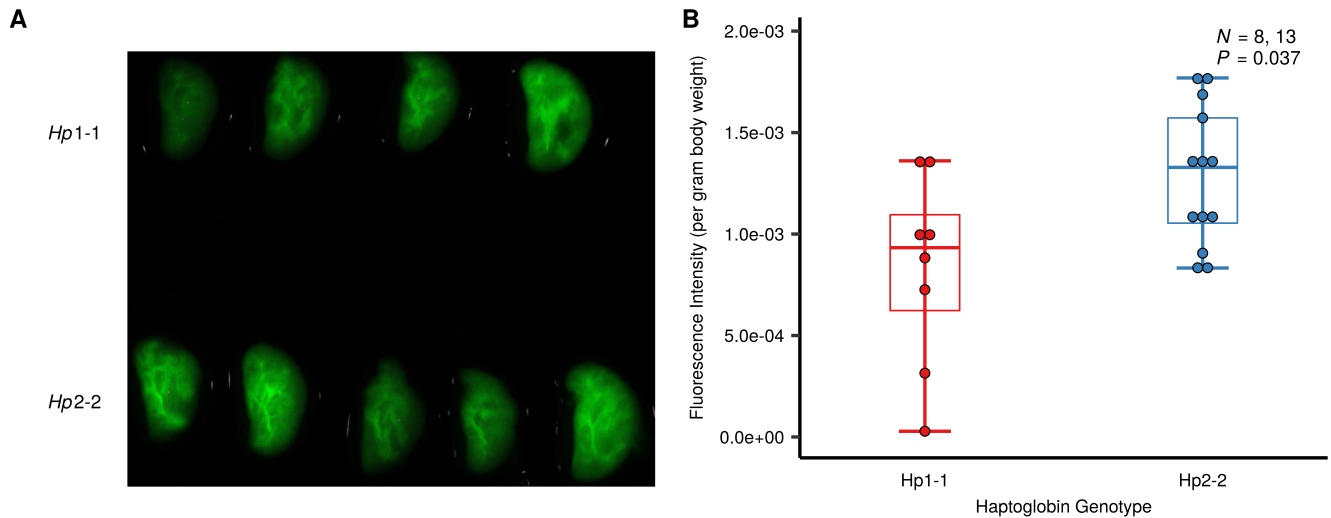


550

551 **Figure 2. *Hp2-2* mice have increased markers of lung inflammation.**

552 *Hp1-1* (red) and *Hp2-2* (blue) mice were treated with CS and IV CFH. (A) Myeloperoxidase
 553 (MPO) activity was measured enzymatically in whole lungs. Reported values are normalized
 554 to the mean value for *Hp1-1* mice. $P = 0.014$ by Mann-Whitney U test. (B) Whole lung mRNA
 555 was extracted for CXCL-1 and expression measured by real-time PCR. Values are reported
 556 as fold-change relative to GAPDH expression. $P = 0.022$ by Mann-Whitney U test. (C) CXCL-
 557 1 protein levels were measured by ELISA in BAL samples. $P = 0.011$ by Mann-Whitney U test.
 558 Dots represent individual values. For the box plots, the horizontal bars represent the median,

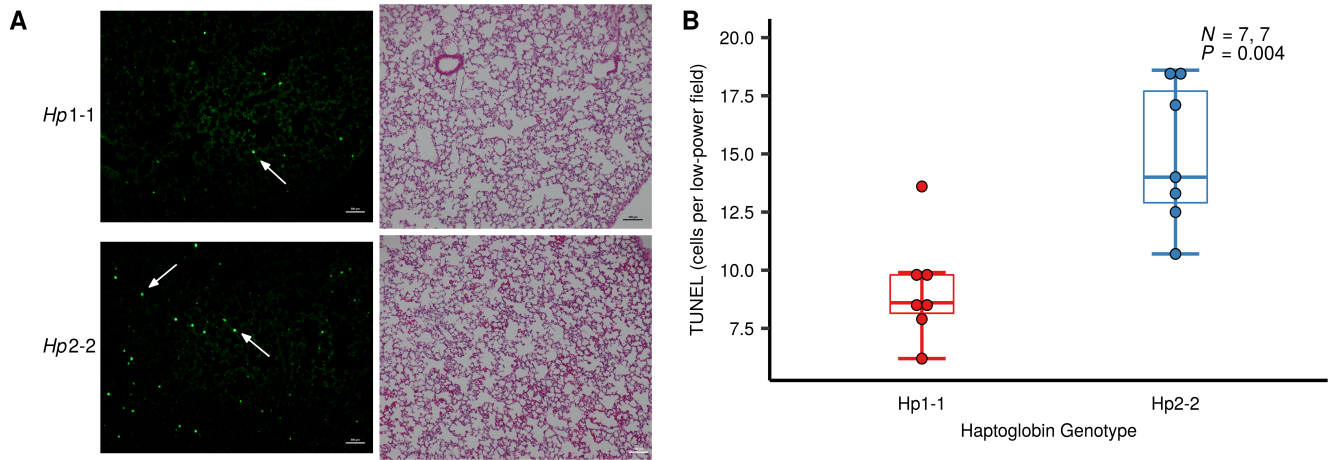
559 boxes represent the interquartile range (IQR, 25th and 75th percentiles), and whiskers
560 represent the minimum and maximum values within $1.5 * \text{IQR}$ from the 25th and 75th
561 percentiles.



562

563 **Figure 3. *Hp2-2* increases lung microvascular permeability.**

564 Angiosense, a fluorescent 70kD macromolecule, was injected retro-orbitally at the time of
 565 treatment. **(A)** After twenty-four hours, whole lungs were excised and imaged using a high
 566 sensitivity CCD camera. **(B)** Fluorescent signal per lung was normalized to body weight and
 567 quantified. Dots represent individual values. For the box plots, thick horizontal bars represent
 568 the median, boxes represent the interquartile range (IQR, 25th and 75th percentiles), and
 569 whiskers represent the minimum and maximum values within 1.5 * IQR from the 25th and 75th
 570 percentiles. * $P = 0.037$ by Mann-Whitney U test.



571

572 **Figure 4. *Hp2-2* mice have increased pulmonary apoptosis**

573 *Hp1-1* and *Hp2-2* mice were treated with CS and IV CFH. Lungs were harvested at 4 hours

574 and examined for apoptotic cells by the TUNEL assay by a trained reviewer blinded to

575 genotype. **(A)** Representative TUNEL stain images (left images) show increased number of

576 TUNEL-positive cells (white arrows) in *Hp2-2* mouse lungs compared with *Hp1-1* mouse

577 lungs. H&E stained sections from the same lung (right images). Scale bars on TUNEL

578 images: 500 μ m, scale bars on H&E images: 100 μ m. **(B)** *Hp2-2* mouse lungs (blue)

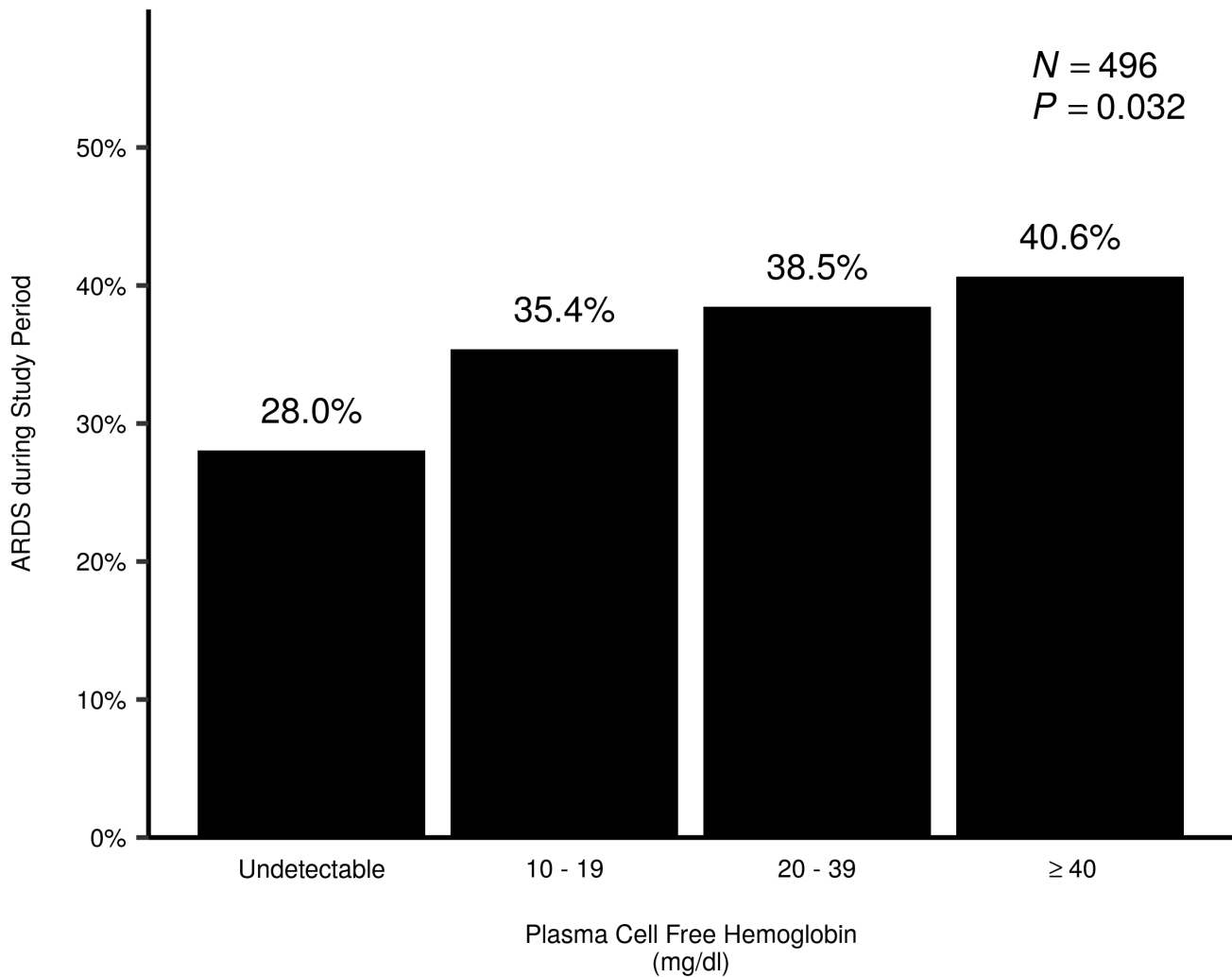
579 demonstrated increased apoptosis of pulmonary cells following sepsis compared with *Hp1-1*

580 mice (red). Dots represent individual values. For the box plots, thick horizontal bars represent

581 the median, boxes represent the interquartile range (IQR, 25th and 75th percentiles), and

582 whiskers represent the minimum and maximum values within 1.5 * IQR from the 25th and 75th

583 percentiles. * $P = 0.004$ by Mann-Whitney U test.



584

585 **Figure 5. ARDS risk increases with higher plasma cell-free hemoglobin during sepsis**

586 Risk of developing ARDS during sepsis increased with higher enrollment plasma CFH levels.

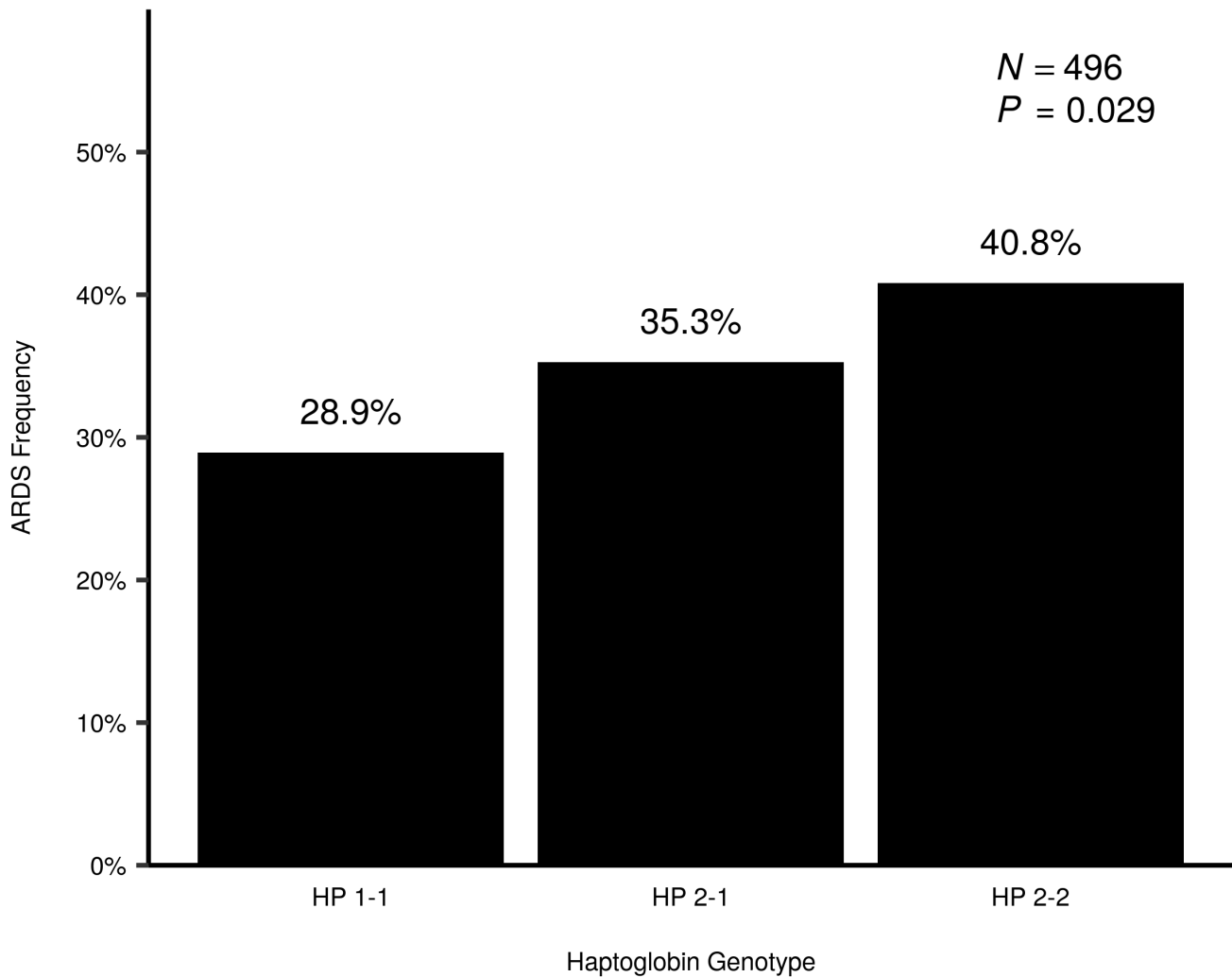
587 Patients are grouped by enrollment plasma CFH quartile, height of bars and numbers over

588 bars indicate percentage of patients who developed ARDS during the study period. Number of

589 patients per quartile = 82, 130, 156, 128 respectively (*N* = 496 in total). *P* = 0.032 by Cochran-

590 Armitage test for trend of increasing ARDS risk ordered by CFH quartile. The lower limit of

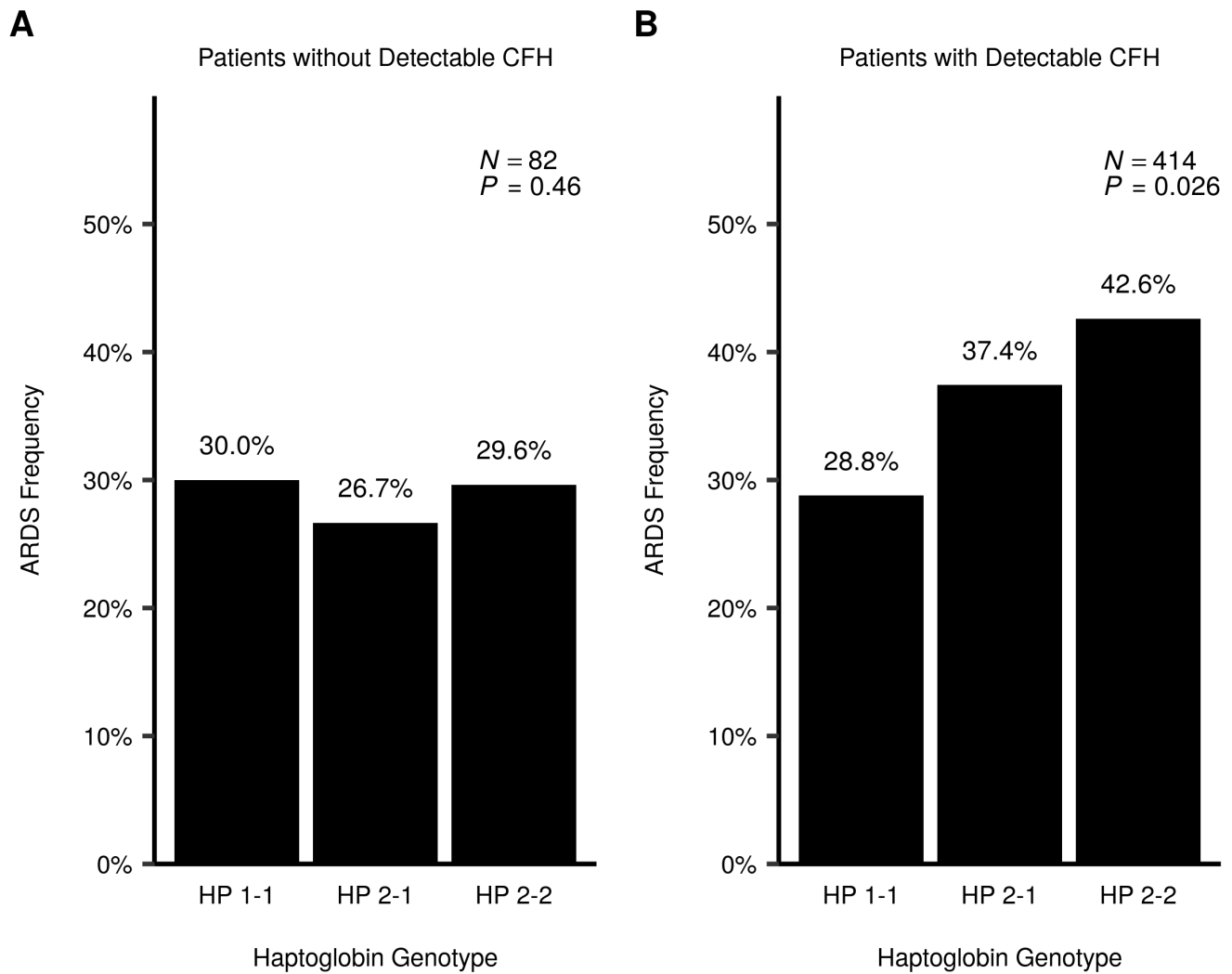
591 detection for the assay is 10 mg/dL.



592

593 **Figure 6. Haptoglobin genotype increases ARDS risk in septic adults**

594 In the entire study cohort ($N = 496$), *HP2-2* patients and *HP2-1* patients had increased risk of
 595 developing ARDS during the study period. Height of bars and numbers over bars indicate
 596 proportion of patients developing ARDS for each group. $P = 0.029$ by Cochran-Armitage test
 597 for increasing risk ordered by number of *HP2* alleles.

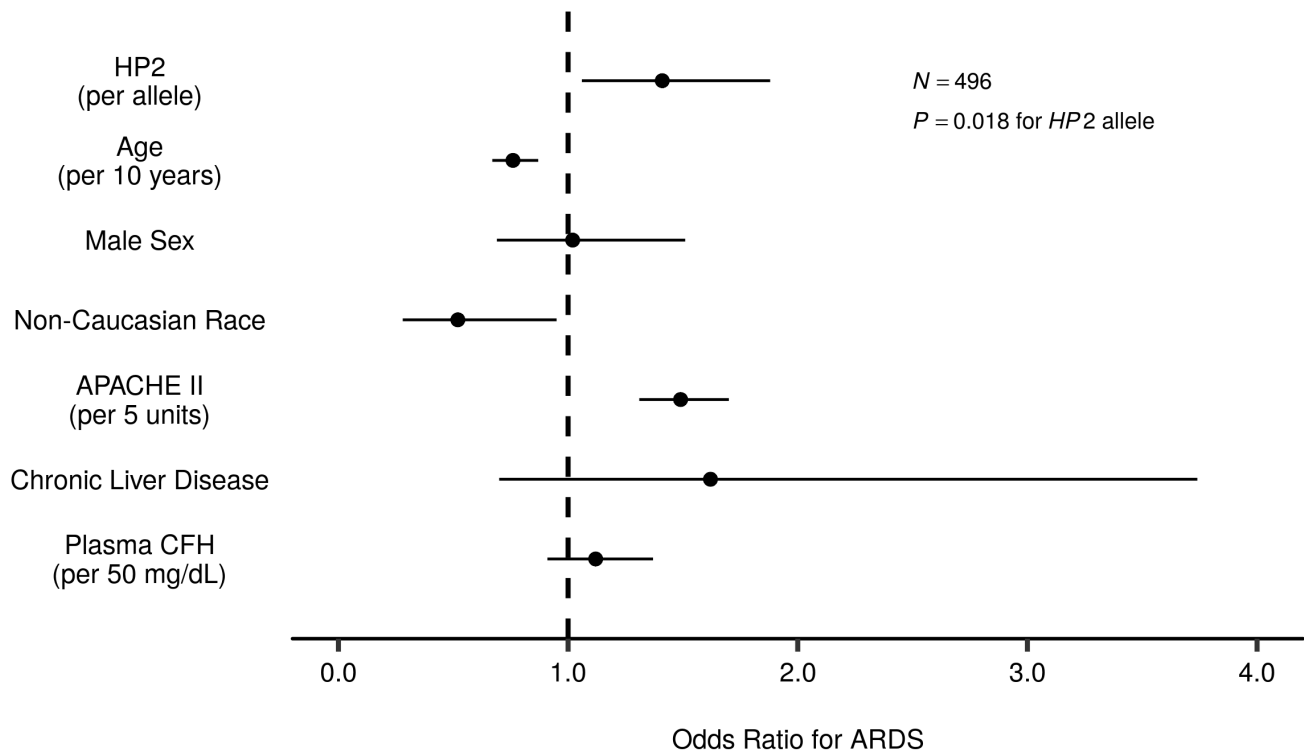


598

599 **Figure 7. Haptoglobin genotype affects ARDS risk only in patients with detectable**
 600 **plasma cell-free hemoglobin.**

601 **(A)** There was no association between *HP* genotype and ARDS risk in patients with
 602 undetectable plasma cell-free hemoglobin (CFH). $N = 82$, $P = 0.46$ by Cochran-Armitage test.

603 **(B)** An association between haptoglobin (*HP*) genotype and ARDS risk was only observed in
 604 patients with detectable CFH. $N = 414$, $P = 0.026$ by Cochran-Armitage test.



605

606 **Figure 8. Haptoglobin 2 variant increases ARDS risk in septic adults when controlling**
 607 **for clinical factors**

608 Multivariable logistic regression model for ARDS in study population (N = 496). Circles

609 represent point estimate odds ratios and horizontal lines represent 95% confidence intervals

610 for each variable included in the model. Black dashed vertical line indicates odds ratio of 1.0

611 (no change in ARDS risk). P = 0.018 for HP2 variant. APACHE II – Acute physiology and

612 chronic health evaluation II. HP2 – Haptoglobin 2. CFH – cell-free hemoglobin.

613 **Tables**614 **Table 1. Demographic and clinical characteristics of study population**

	HP1-1	HP2-1	HP2-2	P^A
Demographics				
Number	76	224	196	
Age (years)	56 (16)	59 (15)	56 (16)	0.077
Male Sex	37 (49%)	117 (52%)	111 (57%)	0.444
Caucasian Race	62 (82%)	193 (86%)	170 (87%)	0.204
Comorbid Medical Conditions				
Chronic Kidney Disease	21 (28%)	40 (18%)	41 (21%)	0.188
Chronic Liver Disease	5 (7%)	16 (7%)	6 (3%)	0.165
Diabetes	23 (30%)	75 (34%)	60 (31%)	0.778
ICU Characteristics				
Mechanical Ventilation on Enrollment	47 (62%)	140 (63%)	128 (65%)	0.793
APACHE II Score	28 (7)	28 (8)	26 (8)	0.066
In-Hospital Mortality	15 (20%)	49 (22%)	42 (21%)	0.925
Ventilator-Free Days	18 (11)	18 (11)	18 (11)	0.918
ARDS During Study Period	22 (29%)	79 (35%)	80 (41%)	0.029 ^B
Brussels Organ Failures on Enrollment				
Circulatory Failure	57 (75%)	162 (72%)	132 (67%)	0.363
Coagulation Failure	12 (16%)	28 (13%)	23 (12%)	0.661
Hepatic Failure	15 (20%)	40 (18%)	36 (18%)	0.935
Renal Failure	29 (38%)	84 (38%)	72 (37%)	0.973
Any Organ Failure	65 (86%)	189 (84%)	158 (81%)	0.487
Plasma Biomarkers				
Plasma Cell-Free Hemoglobin (mg/dL)	20 [10, 50]	20 [10, 30]	20 [10, 30]	0.251
Haptoglobin (µg/dL)	1600 [800, 3880]	1260 [570, 3300]	860 [330, 1940]	0.001

615

616 Data are presented n (%) for categorical variables, mean (standard deviation) for continuous
617 variables with normal distributions, and median [interquartile range] for continuous variables with non-
618 normal distributions.

619 ^AGroup-wise comparison testing performed using Chi-squared test for categorical variables, one-way

620 ANOVA for continuous variables with normal distributions, and Kruskal-Wallis H Test for continuous
621 variables with non-normal distributions. ^BBy Cochran-Armitage test for trend with alternative
622 hypothesis that risk increases with each *HP2* allele.

623 **Table 2. Multivariable logistic regression model of ARDS in septic ICU patients**

Variable	Odds Ratio	95% Confidence Intervals	<i>P</i>
<i>HP2</i> Allele Count	1.41	[1.06; 1.88]	0.018
Age (per 10 years)	0.76	[0.67; 0.87]	< 0.0001
APACHE II (per 5 units)	1.49	[1.31; 1.70]	< 0.0001
Male Sex	1.02	[0.69; 1.51]	0.92
Non-Caucasian Race	0.52	[0.29; 0.95]	0.033
Plasma CFH (per 50 mg/dL)	1.12	[0.91; 1.37]	0.29
Chronic Liver Disease	1.62	[0.70; 3.74]	0.26

624

625 Number of subjects: 496

626 APACHE: Acute Physiology and Chronic Health Evaluation score.

627 CFH: Circulating free hemoglobin. *HP2*: Haptoglobin-2 variant